Volume 1 | Number 1 | Jan 2013 | Pages 1–100

Catalysis
Science &
Technology

www.rsc.org/catalysis

ROYAL SOCIETY
OF CHEMISTRY

This is an *Accepted Manuscript*, which has been through the Royal Society of Chemistry peer review process and has been accepted for publication.

Accepted Manuscripts are published online shortly after acceptance, before technical editing, formatting and proof reading. Using this free service, authors can make their results available to the community, in citable form, before we publish the edited article. We will replace this *Accepted Manuscript* with the edited and formatted *Advance Article* as soon as it is available.

You can find more information about *Accepted Manuscripts* in the **Information for Authors**.

Please note that technical editing may introduce minor changes to the text and/or graphics, which may alter content. The journal's standard **Terms & Conditions** and the **Ethical guidelines** still apply. In no event shall the Royal Society of Chemistry be held responsible for any errors or omissions in this *Accepted Manuscript* or any consequences arising from the use of any information it contains.

www.rsc.org/catalysis

Catalysis Science and Technology

ARTICLE

Galvanic Displacement as a Route to Highly Active and Durable, Extended Surface Electrocatalysts

S.M. Alia,[a] Y. Yan[b,*] and B.S. Pivovar[a,*]

Abstract

Spontaneous galvanic displacement has been utilized in the development of novel electrocatalysts. The process occurs when a less noble metal template contacts a more noble metal cation and combines aspects of corrosion and electrodeposition. The cost of platinum (Pt) limits the commercial deployment of proton exchange membrane fuel cells. Although carbon supported Pt typically has moderate mass activity for oxygen reduction, it is limited by relatively modest specific activity (activity per unit surface area). Conversely, extended Pt surfaces typically have high specific activity for oxygen reduction, but commonly have low surface areas. Catalysts formed by spontaneous galvanic displacement are ideally situated, being able to take advantage of the specific activities generally associated with the catalyst type while significantly improving upon the surface area. In addition to acidic oxygen reduction, spontaneous galvanic displacement has been used in the development of catalysts for variety of electrochemical reactions: hydrogen oxidation; alcohol oxidation; and basic oxygen reduction. Materials for these reactions have been incorporated into this perspective. Spontaneous galvanic displacement is a promising route in catalyst synthesis and in cases these electrocatalysts have demonstrated state of the art performance.

Introduction

The commercial viability of proton exchange membrane (PEM) fuel cells has been limited by the cost of the catalyst layer.[1] Carbon supported Pt nanoparticles (Pt/C), the typical catalysts used in PEM fuel cells, exhibit moderate oxygen reduction reaction (ORR) mass activities in spite of limitations in ORR (area) specific activity due to their relatively high electrochemical surface areas (ECSAs). Carbon supported Pt nanoparticles are typically prone to activity losses in fuel cell operation due to corrosion of the carbon support and Pt aggregation driven by Ostwald ripening, surface tension, and dissolution and migration from the catalyst layer into the PEM.[2,3]

Limitations in the specific ORR activity of Pt nanoparticles have been attributed to a particle size effect.[1, 4] As the particle diameter of Pt nanoparticles is reduced, the prevalence of low coordination edge sites and less active crystal faces (less active for ORR) increases. The surface available Pt atoms (percentagewise) increase with decreasing particle size and a maximum in mass activity is attained at a specified particle size. The ORR activity of Pt nanoparticles is also impacted by Pt-carbon interactions and strain effects that arise at the nanoscale. Particle size effects have further been found for ORR on palladium (Pd) nanoparticles in base, but have not been confirmed or were not found to be a significant a factor in Au (Au) nanoparticles (ORR, in base) or Pt nanoparticles in hydrogen oxidation (HOR, in base, as discussed later in this paper).[5-7]

Extended surface catalysts have benefits beyond nanoparticles in that they typically have about an order of magnitude higher specific activity. A widely recognized example of an extended surface catalyst is 3M's nanostructured thin film (NSTF) catalysts for PEM fuel cells, which have shown promising properties (high activity, exceptional durability).[8, 9] Extended surface catalysts have been investigated with a variety of deposition techniques, however, and they have typically been limited to low surface areas.[8, 10, 11] **Figure 1** shows ECSA and specific ORR activity (i_s) of extended surface catalysts (Pt only NSTF and nanotubes formed by chemical vapor deposition into anodized alumina templates) and Pt/C (high surface area carbon, HSC). Lines of constant mass activity are shown by the contour lines and are the multiplication product of specific activity (activity per surface accessible site) and surface area on a Pt mass

basis (a measure of percentage of total sites surface accessible). As seen in **Figure 1**, extended surface catalysts typically produce specific activities significantly larger than Pt nanoparticles, but lack the surface area required for high mass activity. In contrast, carbon supported Pt nanoparticles demonstrate lower specific activity, but have high surface areas, and produce comparable, moderate mass activity. In order to produce high mass activity catalysts, both highly active sites (high specific activity) and a high percentage of surface available sites (high ECSA) are required. Mass activity is the metric that best addresses the cost versus performance trade-offs of fuel cell catalysts, but is not a perfect metric as it does not consider issues such as mass transfer or ohmic resistances that occur inside fuel cell electrodes or the potential site blocking effects of contaminants that impact low surface area catalysts more than high surface area catalysts. Regardless, increased surface area of extended surface catalysts would best address these concerns and has remained a primary limitation of these materials to date.
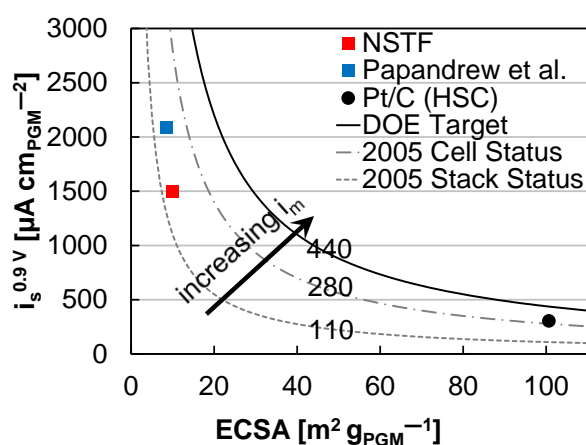

Figure 1. Surface area and specific ORR activities of Pt NSTF, Pt nanotubes formed by chemical vapor deposition (denoted Papandrew et al.), and Pt/C (HSC) in relation to the 2005 PEM fuel cell status and the United States Department of Energy (DOE) target (2015 – 2020).[10-12] The numbers on the 2005 PEM fuel cell status and DOE target lines are the mass activities (i_m, mA mg_{PGM}^{-1}). The arrow within the figure signifies increasing i_m. Surface areas and specific activities were plotted on a Pt group metal (PGM) basis. The NSTF catalyst used in this figure contained only Pt; improvements have since been made to the specific activity and surface area by alloying and synthesis optimization.[8]

Catalysts formed by (spontaneous) galvanic displacement are poised (and in a few cases have shown the ability) to produce high mass activities by: maintaining the high specific activities demonstrated by extended Pt surfaces; and greatly increasing surface area compared to other extended surface catalysts.[13] These galvanically displaced materials share similar characteristics to other demonstrated extended surface catalysts and have shown similar promise in the area of long-term durability to potential cycling. These materials demonstrate benefits in the carbon corrosion regime (> 1.0 V) as might be expected because they avoid the use of carbon. The extended nature of these catalysts also ensures long range conduction independent of individual point contacts (Pt particles on carbon), where carbon corrosion is most likely to occur due to the catalytic function of the Pt particles on the carbon oxidation process.[14] Extended surface catalysts show additional

advantages over nanoparticle catalysts in the Pt dissolution regime (0.6 – 0.9 V). In this typical operating window for fuel cell cathodes, Pt dissolution, migration, and repreciptation occurs. Extended surfaces, unlike nanoparticles, have the potential for high surface areas with less lower coordinated (more dissolution prone) catalyst sites. They also tend to be multiple monolayers thick so that they have better tolerance to Pt dissolution than monolayer core shell catalysts. Lastly, extended surface catalysts allow for the potential of proton conduction across their surfaces without the addition of ionomer or electrolyte and potential losses associated with its presence.

Much of the focus to date for galvanic displacement as an electrocatalyst synthesis route has focused on acidic, hydrogen fuel cells (Pt based catalysts). Galvanic displacement also holds great promise in the development of catalysts for a variety of other electrochemical processes. In hydroxide exchange membrane (HEM) fuel cells, these materials have been studied for activity in ORR and HOR.[15, 16] In direct alcohol fuel cells, these materials have been studied for methanol oxidation activity in acidic electrolytes and for methanol, ethanol, and ethylene glycol oxidation activity in basic electrolytes.[7, 15, 17]

The research to date clearly shows these materials have great promise and in some cases have already demonstrated state of the art electrocatalytic performance. The work discussed here is focused on the development of catalysts for fuel cells. The use of galvanic displacement and extended surfaces is also potentially beneficial for a variety of electrochemical devices, including electrolysis, photoelectrochemical, and chemical synthesis systems.

Spontaneous Galvanic Displacement

Galvanic displacement is a highly promising route for novel catalyst synthesis. Galvanic displacement occurs spontaneously when a metal "template" comes into contact with a more noble metal cation.[18-20] In this case, it is thermodynamically favorable for the more noble metal cation to "steal" electrons from the less noble metal (the nobility of metals follows their standard redox potential, **Table 1**). The galvanic displacement process combines aspects of corrosion of the template metal and electrodeposition of the more noble metal cation. An advantage of galvanic displacement as a synthesis route is that the less noble metal provides a template for the resulting structure. This enables the creation of extended surface catalysts through the implementation of extended structure templates (tubes, wires, plates). The galvanic displacement process also tends to form a continuous layer, beneficial for durability.

Table 1. Standard redox potentials of metals studied in the use of galvanic displacement to form electrocatalysts.

Reaction	E^0 [V vs. RHE]
$Au^{3+} + 3e^- \leftrightharpoons Au$	1.498
$Pt^{2+} + 2e^- \leftrightharpoons Pt$	1.180
$Pd^{2+} + 2e^- \leftrightharpoons Pd$	0.951
$Ag^+ + e^- \leftrightharpoons Ag$	0.800
$Ru^{2+} + 2e^- \leftrightharpoons Ru$	0.455
$Cu^{2+} + 2e^- \leftrightharpoons Cu$	0.340
$Ni^{2+} + 2e^- \leftrightharpoons Ni$	-0.257
$Co^{2+} + 2e^- \leftrightharpoons Co$	-0.280

Galvanic displacement is shown schematically in **Figure 2** as a general case for the displacement of a nanowire by a more noble metal cation. The schematic shows increasing time into displacement, moving from left to right. As an example, a less noble nanowire (for example, Ag depicted in blue) is displaced by higher nobility metal ions (Pt, depicted in red). Depending on reaction variables, different final structures can be obtained; however for full Pt displacement of Ag nanowires, Pt nanotubes are typically obtained. Galvanic displacement allows for the synthesis of catalysts (structures and compositions) which cannot be synthesized directly: that are shape-controlled, including the morphologies of wires, tubes, and plates; and with tuneable compositions. A major advantage of galvanic displacement is the number of tuneable parameters that can be controlled during synthesis (**Table 2**). Experimental results to date (as discussed later in this paper) have shown that relatively minor changes to these variables can have significant impact on observed structures and properties. As galvanic displacement is new, very little of this experimental space has been studied; it seems inevitable that these materials will find further performance improvements and become potentially enabling elements in electrochemical devices.
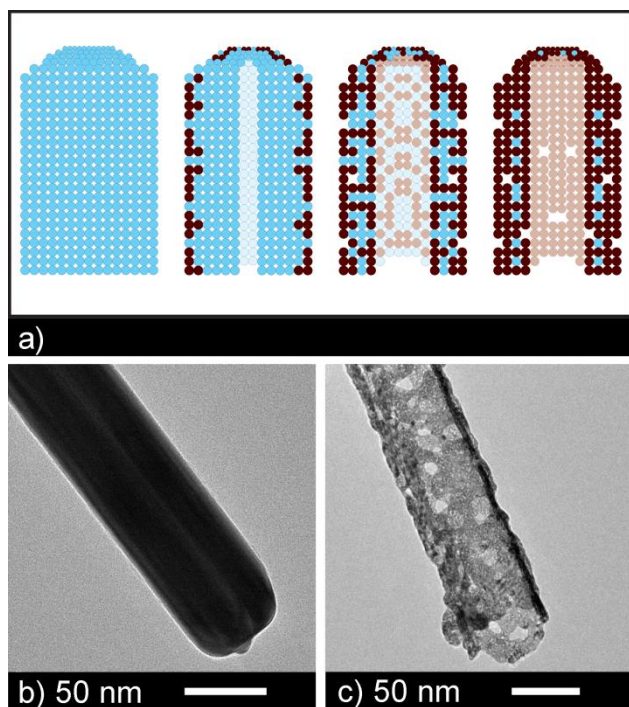
Figure 2. a) Schematic of the displacement process. Transmission electron microscopy images of a b) Ag nanowire and c) corresponding Pt nanotube following galvanic displacement.

Table 2. Experimental parameters examined for spontaneous galvanic displacement in the formation of Pt catalysts.

Parameter	Range
Template morphology	Wire, plate, tube[21-26]
Template metal	Ag, Cu, Ni, Co[21-26]
Degree of displacement	~ 0-100%[21, 25, 26]
Displacement anion	Acetate, chloride[13, 24]
Displacement temperature	20-300°C[22]
Pt Precursor	2+, 4+[7, 13]
Displacement medium	Water, ionic liquid[22]
Template ligand	Various[22]

Through the efforts to develop Pt catalysts by spontaneous galvanic displacement, significant alterations have been made to the metal (Ag, Cu, Ni, Co) and morphology (wire, plate, tube) of the template. Extended morphologies of metals were previously synthesized and identified as potential template candidates for spontaneous galvanic displacement (**Table 3**). For purposes of this discussion, nanowires and nanoplates synthesized by "wet chemistry" (not by hard templates) were considered, with preference given to smaller morphologies (diameter or thickness). The atomic radii of these metals were included since an alloying effect and compressed Pt lattice could potentially improve ORR activity; crystallographic structure was also included since a mismatch (Pt displacing Co) could potentially alter Pt coverage (in partial displacement) or morphology (in full displacement).[27-29] Redox states of the metals with the lowest standard potential were included since displacement stoichiometry could impact morphology.

Table 3. Examined metals and previously synthesized materials of potential templates. For crystallographic structure, face centered cubic (fcc) and hexagonal close packed (hcp) were noted. Redox states are for the metal valences with the lowest standard potential.

Metal	Radius [pm]	Structure	Redox state	Wire diameter [nm]	Plate thickness [nm]
Pt	139	fcc	2	1.3[30]	
Ag	144	fcc	1	10[31]	8.4[18]
Cu	128	fcc	2	85[32]	19.5[33]
Ni	124	fcc	2	60[34]	6[35]
Co	125	hcp	2	150[36]	10[37]

Pt nanowires were also included in **Table 3** to note materials available by direct deposition. Pt nanowires were previously developed and studied for ORR in acid by Wong et al.[30] The materials reported had small diameters (1.3 nm, high surface area) as well as reasonably high specific activity. Although other Pt nanowires and Pt alloy nanowires are available by direct deposition, they result in much larger diameter wires where the surface areas are limited on a mass basis. This catalyst was included due to the wire size and high surface area. Although the Pt nanowires produced a relatively high mass activity, their use as fuel cell catalysts is limited by: the presence of surfactants used during synthesis; durability/structural integrity concerns; and the difficulty of incorporating these materials into membrane electrode assemblies.

As extended surface catalysts have shown exceptional performance on a specific activity and durability basis, generating high surface area materials has remained a barrier that galvanic displacement is well suited to address. Typically, catalysts formed by spontaneous galvanic displacement are larger structures: primarily Pt (or the more noble metal) with outer diameters in the tens of nanometers (full displacement); or core shell (Pt shell with the metal template core, partial displacement) with diameters in excess of 100 nm. Regardless of degree of displacement, hollow Pt structures or thin Pt coatings, these morphologies allow for high surface area materials to be generated. The larger overall nature of the structures (outer diameter, length), however, allows for mechanical stability and durability characteristics not likely attained with direct deposition.

The use of galvanic displacement (in particular partial displacement, or a core shell approach) for the preparation of novel electrocatalysts was highly motivated by the work of Adzic et al. and their significant efforts to develop core shell catalysts. Adzic et al. focused primarily on depositing monolayers using underpotential deposition, followed by galvanic displacement of the monolayers.[38-41] Our approach does not depend on active potential control of the particle surface and is more resistant to durability/performance limitations inherent to monolayers (dissolution and electronic structure effects). The pursuit of galvanic displacement to create extended surface catalysts also leveraged significant recent progress into the areas of the synthesis of extended structure metal nanoparticles with a strong focus on nanowires (**Table 3**).[42]

Electrocatalysis in Acid

The use of galvanic displacement as a catalyst synthesis technique was first reported for PEM ORR.[13] This area has seen the most activity, and has shown great promise as a route to enabling increased mass activity for Pt based electrocatalysis. These efforts started with Ag templated routes and then expanded to include modifications of the synthesis, including the use of other template materials and reaction parameters that have demonstrated improved properties.

Oxygen Reduction – Silver Templated Catalysts

The first efforts into extended surface catalysts based on galvanic displacement started with Ag templates. Pt and Pt-Pd nanotubes were synthesized by the galvanic displacement of Ag nanowires, forming hollow tubes 50 nm in diameter, with walls 4 – 7 nm thick.[13]

Catalysts were electrochemically characterized in rotating disk electrode (RDE) half-cells containing a 0.5 M sulphuric acid electrolyte. In ORR, Pt nanotubes were found to have a specific activity 3.8 times higher than Pt/C (Vulcan) at 0.85 V vs. a reversible hydrogen electrode (RHE). Pt-Pd nanotubes similarly had a specific activity 5.8 times greater than Pt/C (Vulcan) and the highest mass activity of the examined catalysts, ~ 40 % higher than Pt/C (Vulcan). Accelerated durability testing was completed by potential cycling (1000 cycles) 0 – 1.3 V vs. RHE at 60°C. Pt nanotubes retained far greater surface area (~80%) than Pt/C (Vulcan, ~10%) or unsupported Pt nanoparticles (~50%) following durability testing (**Figure 3**).
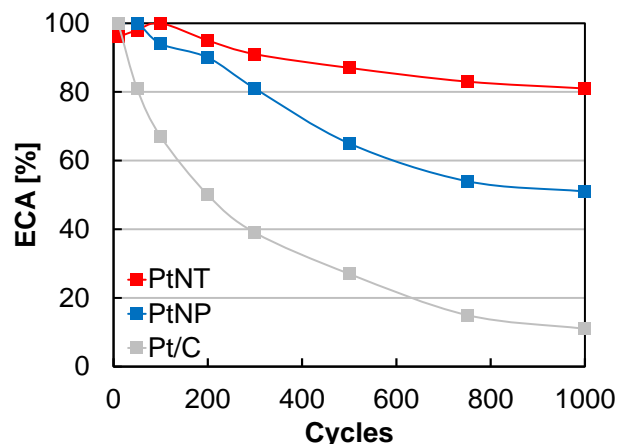

Figure 3. Electrochemical surface area loss (on a percentage basis) of Pt nanotubes, Pt nanoparticles (Pt black, denoted PtNP), and Pt/C (Vulcan) as a function of durability cycles (0.0 – 1.3 V versus RHE).[13] Reprinted (adapted) with permission from Z. Chen, M. Waje, W. Li and Y. Yan, Angew. Chem. Int. Ed., 2007, 46, 4060. Copyright 2007 John Wiley and Sons.

Subsequent efforts with Ag templated nanotubes focused on improving the Pt surface area by adding porosity, by altering the morphology of the Ag templating material, or by reducing the Pt content. Porous Pt nanotubes were synthesized by making alterations to the galvanic displacement procedure, principally in supplying Pt in the form of chloroplatinic acid, thereby forcing Ag precipitation as AgCl. Preliminary studies have begun to examine the role of the Pt precursor, displacement temperature, and concentration on the morphology and activity of Pt nanotubes.[22-24] Although little is conclusively known on the impact of chloride on the mechanism of Pt galvanically displacing Ag, its use appeared to introduce porosity into the nanotube walls, thereby increasing surface area (16.3 to 23.9 m^2 g$_{Pt}$$^{-1}$).

Porous Pt nanotubes were synthesized with an average wall thickness of 5 nm and an outer diameter of 60 nm (**Figure 4**).[7] Catalysts were electrochemically characterized in RDE half-cells containing a 0.1 M perchloric acid electrolyte. Porous Pt nanotubes had a specific ORR activity 3.1 times greater than Pt/C (Vulcan) at 0.9 V vs. RHE. Porous Pt nanotubes also retained a greater percentage of surface area in durability testing (30,000 cycles, 0.6 – 1.1 V vs. RHE), 23.5% loss compared to 48.3% loss (Pt/C (Vulcan)). In terms of ORR mass activity, Porous Pt nanotubes improved 6.8% following durability testing; Pt/C (Vulcan), in comparison, lost 94.7% of its initial ORR mass activity.
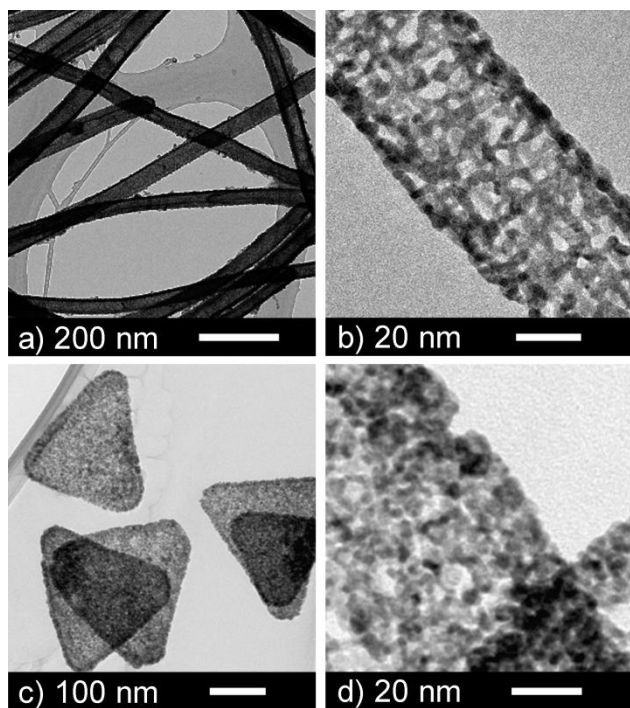
Figure 4. Transmission electron microscopy images of a-b) porous Pt nanotubes and c-d) Pt nanoplates.[7] Reprinted (adapted) with permission from S. Alia, G. Zhang, D. Kisailus, D. Li, S. Gu, K. Jensen and Y. Yan, Adv. Funct. Mater., 2010, 20, 3742. Copyright 2010 John Wiley and Sons.

While most work to date has focused on wires or tubes, Pt nanoplates were synthesized by the galvanic displacement of Ag nanoplates.[43] Although the nanoplates are significantly shorter than the nanowires or nanotubes (hundreds of nanometers as opposed to several micrometers), the specific ORR activities offer sizeable advantages to nanoparticles and exhibited properties similar to other galvanically displaced extended surface catalysts presented here. As in the case of porous Pt nanotubes, Pt nanoplates used a chloride Pt precursor (potassium tetrachloroplatinate); similar surface roughness (porosity) was observed irrespective of template morphology (**Figure 4**). X-ray diffraction (XRD) patterns found a Pt (111) reflection noticeably larger in intensity relative to the Pt (200) reflection (compared to bulk Pt metal with random grain orientation). The difference in intensity suggested preferential growth through templating by the Ag nanoplates. The results suggested that there was some preference for Pt growth direction but final displacement products were less oriented than the Ag nanoplate template materials. In electrochemical testing (RDE half-cells, 0.1 M perchloric acid electrolyte), Pt nanoplates outperformed Pt/C (HSC) in specific ORR activity by 3.7 times. The surface area of the Pt nanoplates, however, was still comparatively low ($15 m^2 g_{Pt}^{-1}$) and the mass activity was lower than Pt/C (HSC, 55%).

Pt coated Pd nanotubes were studied in an effort to reduce the amount of Pt in the nanotubes (replacing subsurface Pt with Pd), thereby increasing the Pt normalized surface area and mass activity for ORR (**Figure 5**).[44] Pt coated Pd nanotubes were synthesized by displacing Ag nanowires with Pd, then partially displacing the formed Pd nanotubes with Pt. Although Pd is a PGM, its metal price ($ 392.95 t oz^{-1}, five year average) is 28% the metal price of Pt ($ 1414.68 t oz^{-1}, five year average). To incorporate the difference in metal prices, a cost weighted metric was used to evaluate catalyst activity in which the Pt coated Pd

nanotubes exceeded the DOE mass activity target on a cost-normalized basis.

Oxygen Reduction – Beyond Silver Templates

Ag was originally the focus of templates for catalysts synthesized by spontaneous galvanic displacement since Ag nanowires and nanoplates were relatively established materials and allowed for the study of a wide range of system parameters. Ag, however, is generally disadvantageous as a catalyst template since residual Ag can migrate through the membrane and plate onto the anode impacting performance.[23] Ag also has a relatively high redox potential (0.800 V vs. RHE) and can be difficult to remove electrochemically from Pt. Ag further has a lattice constant larger than that of pure Pt, potentially disadvantageous as an alloy since a larger Pt lattice could potentially decrease the specific activity of Pt ORR. Later efforts in the development of extended surface ORR catalysts, therefore, moved away from Ag.

Cu nanowires were utilized as a Pt template due to the ease of electrochemical dissolution (0.340 V vs. RHE) and since the lattice constant was slightly compressed relative to Pt. Cu templated Pt nanotubes and Pt coated Cu nanowires were respectively synthesized by the complete and partial galvanic displacement of Cu nanowires.[45] Pt coated Cu nanowires were synthesized with a diameter of 100 nm and a Pt content of 18 wt.%; Cu templated Pt nanotubes were synthesized with an outer diameter of 100 nm and a wall thickness of 11 nm. Pt coated nanowires were further found to template the growth directions of the Cu nanowires and to have a compressed lattice in comparison to pure Pt.

Pt coated Cu nanowires and Cu templated Pt nanotubes produced specific ORR activities of greater than 1500 $\mu A cm_{Pt}^{-2}$, 6.2 times greater than Pt/C (Vulcan). The Cu nanowire templates used in these studies were thicker in diameter than the Ag nanowires reported previously (100 nm as opposed to 60 nm). For the reaction conditions investigated, the resulting Cu template nanotubes had thicker walls (11 nm as opposed to 5 nm) and lower surface area (5.6 $m^2 g_{Pt}^{-1}$ as opposed to 16.3 $m^2 g_{Pt}^{-1}$). The Cu templated Pt nanotubes, therefore, produced a relatively low mass activity in ORR (61% of Pt/C (Vulcan)). The synthesis of Pt coated Cu nanowires was needed to reduce the Pt content, thereby increasing the Pt normalized surface area and mass activity. During synthesis, lowering the amount of Pt precursor served to reduce the Pt content, improving Pt utilization, surface area (30.6 $m^2 g_{Pt}^{-1}$), and ORR mass activity (455.3 $mA mg_{Pt}^{-1}$). By improving surface area, Pt coated Cu nanowires thereby exceeded the DOE target for mass activity (by 3.5 %). Following durability testing (30,000 cycles, 0.6 – 1.1 V vs. RHE), Pt coated Cu nanowires also retained high mass activity for ORR (93.6 % of the DOE target).

While Cu template catalysts offered some mass activity advantages over Ag templated catalyst, Cu, like Ag, is likely to migrate from the cathode and plate onto the anode during PEM operation due to its relatively high redox potential (0.34 V vs. RHE). Nickel (Ni) and cobalt (Co) have been more recently explored as templates in part because their redox potentials (Ni - 0.257, Co -0.280 V vs. RHE) are below the onset of HOR, and therefore are not expected to suffer from anode plating in the same way as Ag or Cu. As with Cu, Ni and Co could potentially benefit Pt activity by providing a metal alloying effect. By partially displacing Ni and Co nanowires with Pt, thin coatings were formed on the nanowire surface. Varying the amount of Pt precursor during displacement allowed for the study of catalysts with a wide range of compositions.

Pt coated Ni nanowires (3.8 – 96.8 wt. % Pt) were examined as ORR electrocatalysts.[21, 25] The Ni template included a thin oxide coating, limiting displacement to a relatively low level (16.4 wt.% Pt) even at high Pt reactant concentrations. Higher levels of displacement could be reached by addition of acid during synthesis, presumably to help etch an otherwise protective oxide layer. Through the addition of acid, fully displaced samples (96.8 wt. % Pt) formed hollow nanotubes with walls 20 – 60 nm thick. At low displacement levels, however, Pt was largely constrained to the nanowire surface in a "core-shell" type structure (**Figure 5**).

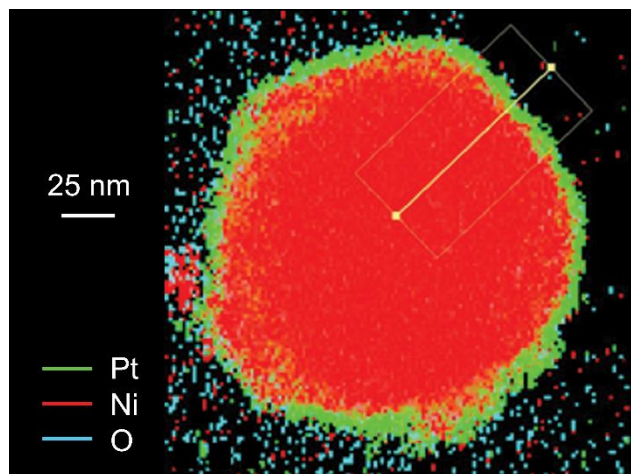
Figure 5. Energy dispersive x-ray spectroscopy map of cross sectioned Pt Ni nanowires (9.6 wt. % Pt) in scanning transmission electron microscopy.[25] Reprinted (adapted) with permission from S. M. Alia, B. A. Larsen, S. Pylypenko, D. A. Cullen, D. R. Diercks, K. C. Neyerlin, S. S. Kocha and B. S. Pivovar, ACS Catalysis, 2014, 4, 1114. Copyright 2014 American Chemical Society.

The Pt coated Ni nanowires produced a wide range of specific ORR activities (850 – 2087 μA cm_{Pt}^{-2}), up to 6.9 times larger than Pt/C (HSC). Large Pt normalized surface areas were found in the case of the Ni nanowires, exceeding 90 m^2 g_{Pt}^{-1}. This high surface area had not been approached previously in a 3-dimensional, extended structure catalyst and marked a significant breakthrough. The ability to utilize Pt this efficiently greatly increased the potential of this class of catalysts. The highest ORR mass activity produced (917 mA mg_{Pt}^{-1}) outperformed Pt/C (HSC) 3.0 times and exceeded the DOE target 2.1 times. Following durability testing (30,000 cycles, 0.6 – 1.0 V vs. RHE), the highest ORR mass activity (661 mA mg_{Pt}^{-1}) was still 49% higher than the DOE target (2.9 times greater than Pt/C (HSC)). These durability studies also showed that the Ni nanowire "core" remained intact throughout potential cycling presumably due to the Pt, Ni oxide layer that protected the metallic Ni core.[25] Depending on the conductivity and thickness of the oxide layer, this architecture can be greatly advantageous in electrocatalytic applications as the metallic core of the wire has high conductivity and is continuous over many microns alleviating any electronic conductivity issues that might occur within the catalyst layer or in connection to individual particles. While the role of the oxide layer is still being explored, its presence represents another variable that can possibly be tuned for improved properties.

Co nanowires were also investigated as galvanic displacement templates and provide interesting comparisons to the Ni nanowire system. Pt coated Co nanowires were synthesized with a Pt composition between 2.1 to 67.7 wt. %.[21, 26] Although the Co wires also exhibited an oxide layer, the impact of the oxide layer on the Co nanowires was different than that observed for the Ni nanowires. During displacement, the oxide layer on the Co nanowires did not limit Pt displacement to the very low levels observed for Ni nanowires in the absence of added acids. The specific activities of Pt Co nanowires for ORR increased as the Pt content decreased, from 2053 μA cm_{Pt}^{-2} (67.7 wt. % Pt) to 2783 μA cm_{Pt}^{-2} (4.5 wt. % Pt) (**Figure 6**). XRD patterns confirmed an increasingly compressed Pt lattice over the composition range examined, potentially contributing to the high specific ORR activity. This high specific activity and shifting of Pt XRD peaks was not observed in the Pt Ni nanowires. Unfortunately, the Pt surface areas obtained for the Co displaced samples were substantially lower (maximum ECSA of 29.1 m^2 g_{Pt}^{-1}) than those obtained for Ni nanowires. Still, Pt Co nanowires produced a maximum ORR mass activity (793 mA mg_{Pt}^{-1}) 79% greater than the DOE target (2.6 times Pt/C (HSC)). Following durability testing (30,000 cycles, 0.6 – 1.0 V vs. RHE), Pt Co nanowires produced a maximum ORR mass activity (579 mA mg_{Pt}^{-1}) 30% greater than the DOE target (2.6 times Pt/C (HSC)). The durability studies of these materials also showed a strong contrast to the Ni nanowire templated materials in that upon exposure to acid, the Co nanowire "core" was immediately etched away leaving only a Co containing Pt freestanding "shell" (nanotube) as the active catalyst material.
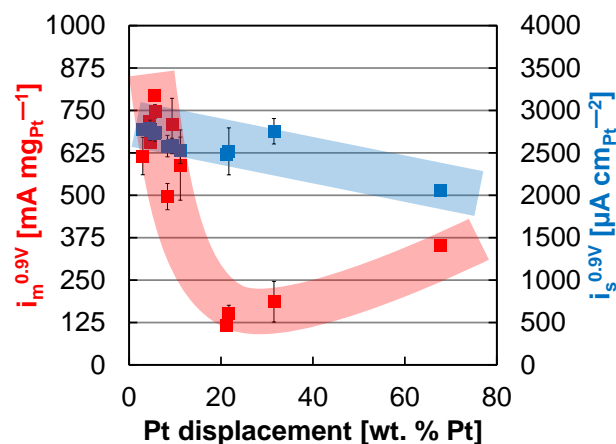

Figure 6. Mass and specific ORR activities of Pt Co nanowires as a function of percent Pt displacement.[26] Reprinted (adapted) with permission from S. M. Alia, S. Pylypenko, K. C. Neyerlin, D. A. Cullen, S. S. Kocha and B. S. Pivovar, ACS Catalysis, 2014, 4, 2680. Copyright 2014 American Chemical Society.

A summary of relevant ORR catalyst activities at 0.9 V vs. RHE in a 0.1 M perchloric acid electrolyte are presented (**Figure 7**). Activities in terms of i_s are plotted against ECSA. Mass activity for ORR is the specific activity multiplied by the surface area. Values of constant mass activity follow contour lines, and the solid black line denotes the DOE 2020 mass activity target (440 mA mg_{PGM}^{-1}). Catalysts to the upper right of this line exceed the DOE target. Conventional carbon supported Pt nanoparticle catalysts produce a high surface area, low specific activity, and moderate mass activity. The target performance for advanced electrocatalysts consists of high specific activity (like that obtained for PtCo, Pt coated Co nanowires) and high surface area (like that obtained for PtNi, Pt coated Ni

nanowires). While many of the initial galvanically displace materials (from Ag or Pd) did not demonstrate high mass activities, shifting the template materials to Cu, Ni, and Co allowed for the Pt surface area to increase and the mass activity to exceed the DOE target. The potential for developing materials that exhibit both high specific activity and ECSA in a single material strongly exists and would represent a further improvement in mass activity compared to traditional carbon supported Pt nanoparticles.
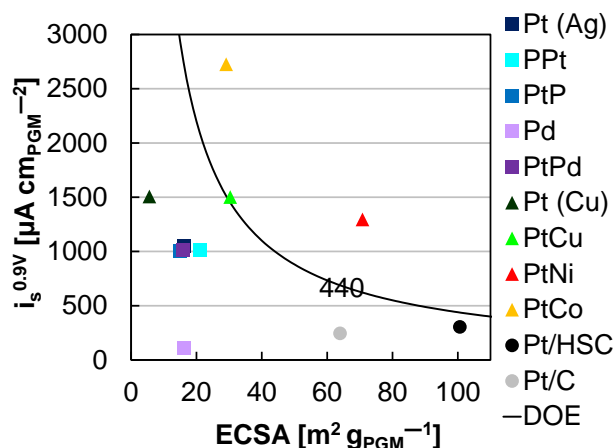

Figure 7. Survey of catalyst ECSAs and specific ORR activities on a PGM basis. Catalyst classes were divided between Ag templated (squares), alternative metal templated (Cu, Ni, Co in triangles), and nanoparticle (circles) materials. Ag templated catalysts include Pt nanotubes (Pt (Ag)), porous Pt nanotubes (PPt), Pt nanoplates (PtP), Pd nanotubes (Pd), and Pt coated Pd nanotubes (PtPd). Alternative metal templated catalysts include Cu templated Pt nanotubes (Pt (Cu)), Pt coated Cu nanowires (PtCu), Pt coated Ni nanowires (PtNi), and Pt coated Co nanowires (PtCo). Nanoparticle catalysts include commercial benchmarks Pt/C (HSC, denoted Pt/HSC in figure) and Pt/C (Vulcan, denoted Pt/C in figure). The number on the DOE target line (denoted DOE in figure) is the mass activity (i_m, mA mg$_{PGM}^{-1}$).

Beyond the mass activity benefits demonstrated by these novel galvanically displaced electrocatalysts, these materials have also shown improved durability (characteristic of extended surface electrocatalysts) in comparison to conventional carbon supported Pt, both in terms of surface area (on a percentage retention basis) and ORR activity. Extended surface electrocatalysts eliminate the need of the carbon support to provide electronic continuity and "dilute" Pt within the electrode layer. The removal of carbon helps to reduce corrosion issues. Extended Pt surfaces also largely avoid surface area loss from agglomeration since they start with longer length scale features. Surface area and activity losses (and ORR mass activity losses) are observed in the Cu, Ni, and Co nanowires partially displaced with Pt. These losses may be related to the susceptibility of the transition metal to dissolve during potential cycling and require further study, but still result in materials that maintain performance (post-durability testing).

The performance and durability reported for galvanically displaced electrocatalysts in this section has been obtained for RDE studies. RDE measurements represent model systems where catalytic activity can in theory be obtained free of concerns of mass transport and ion/electron resistance. In fuel cells, catalysts need to be fabricated into high performance electrodes. Unlike carbon supported Pt catalysts which have been extensively optimized in fuel cell electrodes, the extended surface catalysts have seen almost no such developmental effort and suffer from much higher density and different dispersion characteristics when mixed into inks used for electrode fabrication that include polymer electrolytes for ion conduction. Optimizing the performance of the galvanically displaced catalysts presented here and capitalizing on their high mass activity and durability in fuel cells remains an active research area in need of further advances.

Alcohol Oxidation

Catalysts for direct alcohol fuel cells were also developed using galvanic displacement. Although not suited for the transportation sector, the use of a liquid fuel and the relatively high volumetric energy densities of alcohols are advantageous for smaller applications including portable electronics and small vehicles. In comparison to hydrogen-based fuel cells, however, direct alcohol fuel cells have additional kinetic losses at the anode due to the overpotential associated with alcohol oxidation.

The effect of extended metal surfaces in these reactions and conditions is not as extensively studied as ORR in PEM fuel cells. Catalysts synthesized by galvanic displacement, however, can potentially benefit by similar mechanisms. For many of these reactions, particle size effects have been observed on a variety of metals. Lattice strain has been found to affect the activities of metals in these reactions as well. Galvanic displacement provides the presence of extended surfaces, structural tuning, and can provide high surface areas. While these attributes can benefit activity in hydrogen-based fuel cells, it is potentially useful in alcohol oxidation reactions as well.

Porous Pt nanotubes, previously presented as acidic ORR catalysts, were also studied for methanol oxidation.[7] The nanotubes produced a peak specific activity for methanol oxidation 2.0 times greater than Pt/C (Vulcan). Although these catalysts produced similar onset potentials, porous Pt nanotubes oxidized carbon monoxide at a lower potential (beneficial in intermediate poisoning) and retained a higher percentage of activity following chronoamperometric testing (a measure of intermediate poisoning effects).

Pt ruthenium and Pt tin coatings on Cu nanowires were synthesized by partial displacement. Pt ruthenium coated Cu nanowires were formed by the simultaneous displacement of Cu with Pt and ruthenium.[17] Pt tin coated Cu nanowires were formed by the partial displacement of Cu with Pt and the subsequent reduction of tin in the presence of the nanowires. The synthesized nanowires had an onset potential for methanol oxidation lower than carbon supported Pt ruthenium nanoparticles (PtRu/C, **Figure 8**). The Pt ruthenium nanowires further outperformed the nanoparticles on a mass activity basis throughout the low overpotential region (0.3 – 0.5 V vs. RHE). Pt ruthenium nanowires also retained higher activity following durability testing (30,000 cycles, 0.0 – 0.5 V vs. RHE) than the Pt ruthenium nanoparticles and Pt tin nanowires.
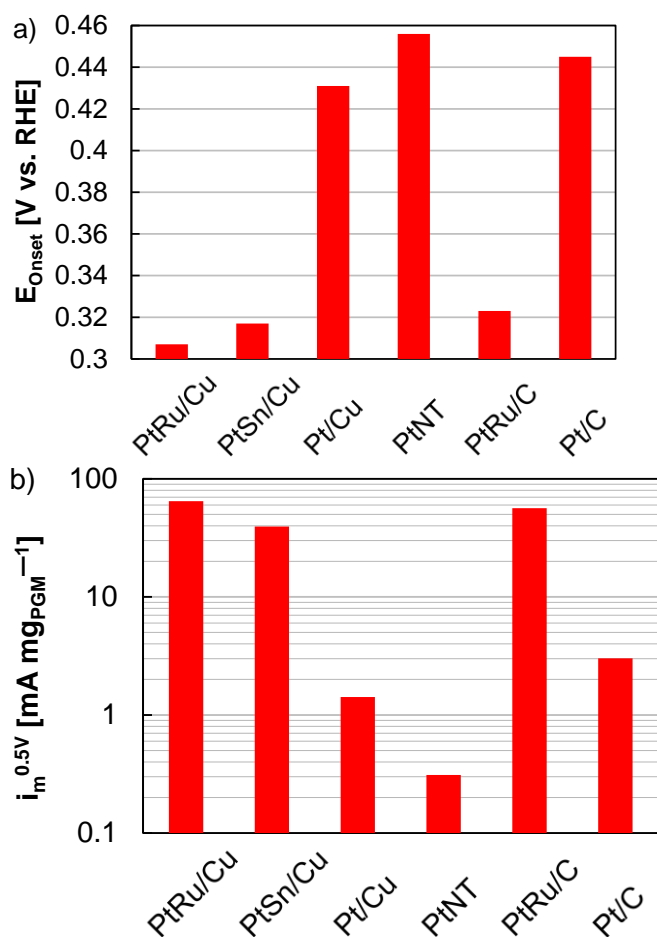
Figure 8. Methanol oxidation mass activities of Pt ruthenium coated Cu nanowires (PtRu/CuNW), Pt tin coated Cu nanowires (PtSn/CuNWs), Pt coated Cu nanowires (Pt/CuNW), Pt nanotubes (PtNT(Cu)), PtRu/C, and Pt/C (Vulcan).[17]

Electrocatalysis in Base

While most of the work developing advanced electrocatalysts for fuel cells has focused on proton exchange membranes, hydroxide exchange membrane fuel cells (HEMFCs) have emerged as a potentially viable fuel cell device, primarily due to the fact that non-PGMs are stable in base and so it becomes possible to eliminate the use of Pt in the catalyst layers, thereby reducing unit cost.[46] Challenges remain in the efforts to commercialize HEMFCs, including the need to form highly conductive, durable membranes, soluble ionomers, and highly active catalysts for ORR and HOR. Although Pt can be avoided in HEMFCs, few catalysts have exceeded the activity of Pt in either alkaline ORR or HOR. HOR also adds a catalyst development challenge typically not a concern in PEM fuel cells. While Pt ORR activity is similar in acid and base, HOR is two orders of magnitude slower on Pt in base than in acid.[7, 47, 48] In alkaline ORR, Ag is generally seen as a promising catalyst, with a significantly lower metal cost and a specific activity within an order of magnitude of Pt.[49] Further progress, however, is needed in this area to bridge the activity gap and provide catalysts with high mass activity for ORR in HEMFCs. The catalyst advances and approaches presented here are also of potential interest for more traditional alkaline fuel cells based on aqueous potassium hydroxide.

Oxygen Reduction

Ag nanowires were studied as ORR catalysts in base and were synthesized by direct deposition. Although not formed by galvanic displacement, the Ag nanowires offer similar specific activity benefits and were later used as a template for ORR catalysts in base (Pd nanotubes and Au nanotubes, as discussed later in this paper). Future improvements of Ag ORR catalysts can be accomplished by the galvanic displacement of less noble metals such as Cu, Ni, and Co. Galvanic displacement would likely improve the surface areas of Ag nanowire catalysts and could potentially improve the specific activity as well through an alloying (electronic effect, not necessarily lattice induced) or bifunctional effect.

Ag nanowires were synthesized with a variety of diameters (25 – 60 nm) and studied for ORR.[50] Although the ORR specific activity of Ag nanoparticles increased with diameter, the nanowire activity decreased with increasing diameter (**Figure 9**). The increase in specific activity was potentially due to the shortening of the wires, thereby increasing the proportion of the more active {110} facet.[51] Changes in specific activity were also potentially due to strain effects related to diameter altering the lattice at the surface (surface tension). The high specific activity of the Ag nanowires (25 nm) allowed for a mass activity 16% greater than Ag nanoparticles (2.4 nm) while only having 22% of the surface area.
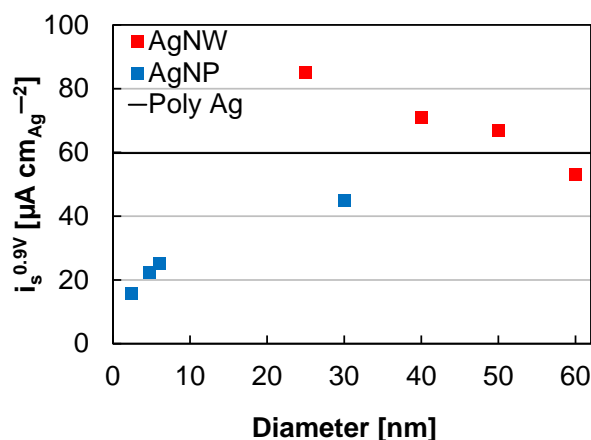

Figure 9. Specific ORR activities of Ag nanowires (AgNW), Ag nanoparticles (AgNP), and a polycrystalline Ag electrode (Poly Ag) at 0.9 V vs. RHE in relation to catalyst size.[50] Reprinted (adapted) with permission from S. M. Alia, K. Duong, T. Liu, K. Jensen and Y. Yan, ChemSusChem, 2012, 5, 1619. Copyright 2012 John Wiley and Sons.

Pd nanotubes were formed by the galvanic displacement of Ag nanowires.[15, 52] Pd nanotubes were studied for ORR activity and exceeded the specific activity of carbon supported Pd nanoparticles (Pd/C) by 3.4 times (within 3% the mass activity). The activity of the Pd nanotubes was primarily attributed to the extended surface, avoiding a Pd particle size effect.[5]

Au nanotubes were also formed by the galvanic displacement of Ag nanowires.[15, 52] Au nanotubes exceeded the specific activity of carbon supported Au nanoparticles by 2.3 times, likely in part due to the use of extended surfaces. The Au nanotubes also exceeded the surface area of the Au nanoparticles due to the

tube wall thickness (6 nm, 19.3 m^2 g$_{Au}$$^{-1}$) relative to the particle size (10 – 30 nm, 2.7 m^2 g$_{Au}$$^{-1}$). In terms of mass ORR activity, the nanotubes exceeded the nanoparticles by 16.3 times. Au nanotubes followed the growth directions of the Ag nanowire template; unlike Pt and Pd, the Au nanotubes appeared to form a highly ordered, smooth, {100} dominant surface which potentially improved ORR activity.[53-55]

Examinations of ORR catalysts in base concluded that among polycrystalline metals, activity decreases in the order: Pt > Pd > Au, Ag.[15, 50, 52, 56] By studying Pd, Au, and Ag catalysts in base, their activities are far closer to Pt than in acid (particularly Ag, Au). As the lowest cost catalyst of these metals, Ag seems to have the most merit in alkaline ORR.[49, 50]

Hydrogen Oxidation

Investigations of catalysts for ORR and alcohol oxidation reactions typically report activity at a specified potential.[1, 57] RDE experiments are also typically not used to report HOR activities in acid since the kinetics are faster than the transport limitations of a liquid electrolyte (Nerstian diffusion limited overpotential).[47] HOR activities in base, however, can be quantified by RDE and are typically reported as exchange current densities since: catalysts typically reach the diffusion limited current at a low overpotential (50 mV); and a potential based metric has yet to be established.[7]

Pt based catalysts, which had been synthesized for acidic ORR, were also investigated for their applicability to HOR in base. As discussed previously, Pt coated Cu nanowires were synthesized by the partial displacement of Cu, forming wires that were 16 wt. % Pt with an outer diameter of 100 nm.[16] The Pt coated Cu nanowires were studied for HOR and exceeded the mass exchange current density of Pt/C (Vulcan) by 89% (3.5 times the specific activity, **Figure 10**). Pt nanotubes also exceeded the specific activity of Pt/C (Vulcan, 2.8 times), but produced lower mass activity due to low surface area. A Cu alloying effect potentially contributed to the high HOR activity.[58]

This work was also influenced by Markovic et al. who studied the role of hydroxyl adsorption, finding that the addition of oxophilic species improved HOR activity beyond Pt.[59] The presence of surface Cu (stable in base), particularly on the Pt coated Cu nanowires, potentially contributed to the high activity. These results were verified on polycrystalline Pt, where the addition of small amounts of Cu (partial atomic layers by underpotential deposition) improved activity.
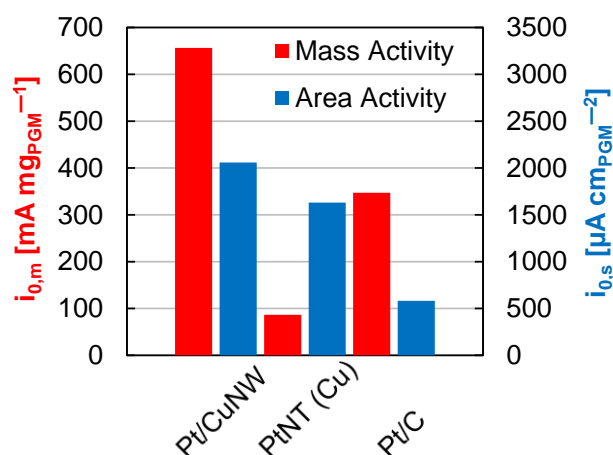

Figure 10. HOR mass and specific exchange current densities of Pt coated Cu nanowires, Pt nanotubes (using a Cu nanowire template), and Pt/C (Vulcan).[16] Reprinted (adapted) with permission from S. M. Alia, B. S. Pivovar and Y. Yan, J. Am. Chem. Soc., 2013, 135, 13473. Copyright 2013 American Chemical Society.

Alcohol Oxidation

HEMs can also be used in direct alcohol fuel cells in place of PEMs, to potentially allow for the use of non Pt catalysts in alcohol oxidation and ORR and by reducing the electro-osmotic drag and permeation rate of alcohol through the membrane.[60, 61]

Pd nanotubes, previously discussed as alkaline ORR catalysts, were also examined for alcohol oxidation activity.[15, 52] In methanol, ethanol, and ethylene glycol oxidation, Pd nanotubes dramatically outperformed Pd/C. In each reaction, Pd nanotubes required an onset potential 150 – 200 mV less and produced specific activities at least an order of magnitude greater in the low overpotential region. Pd nanotubes further required a lower onset potential than PtRu/C (acidic benchmark catalyst) in methanol and ethylene glycol oxidation.

Conclusions

Extended surface catalysts offer a benefit to nanoparticles in that they typically produce specific activities an order of magnitude greater. Catalysts comprised of extended surfaces further provide long range conduction independent of point contacts and have provided durability benefits in the carbon corrosion (avoids carbon) and metal dissolution (less lower coordinated catalyst sites which are prone to dissolution) regimes. Although a variety of deposition techniques have been examined, extended surface catalysts have typically been limited in mass activity due to low surface areas.

Galvanic displacement is a highly promising route to produce high mass activities by maintaining the high specific activity of extended surface catalysts and significantly improving the electrochemically accessible surface area. Galvanic displacement can be used to control the shape and composition of catalysts which cannot be synthesized directly. An advantage of galvanic displacement is a high number of tuneable parameters; relatively small changes to synthesis variables have been found to significantly alter the structures and properties of these catalysts.

Galvanic displacement has been used in the synthesis of catalysts for ORR, HOR, and alcohol oxidation. In each reaction

(particularly ORR), catalysts formed by galvanic displacement produced high mass activities, demonstrating significant benefits to nanoparticle benchmarks. Although galvanic displacement contains many tuneable parameters, most of these studies focused on the template metal and catalyst composition. Much of the possible experimental space for the synthesis of these materials remains to be studied; continuing developments will likely further improve performance, potentially enabling electrochemical devices.

For ORR in acid, catalysts synthesized by galvanic displacement have shown both high specific activities and surface areas, in certain cases (Pt Ni and Pt Co nanowires) more than doubling the DOE mass activity target. Future development of these materials aims to achieve both within the same system: either by using catalysts with high specific activities and thinning the Pt layer (improving surface area); or by using materials with high surface areas and introducing Pt / template metal interactions (potentially improving specific activity). Further advancements in catalyst post-synthesis processing are required to improve the durability of the highest performing materials, which in some cases are greater than 80 wt. % of the template transition metal (Ni, Co, or Cu). Currently, little of the experimental space in the formation of Pt ORR catalysts (Table 2) has been explored; further development of these materials may allow them to become enabling elements in PEM fuel cells.

Although these catalysts have demonstrated great potential for ORR activity in RDE half-cells, this potential has yet to be fully realized in the fuel cell device. The successful implementation of extended surface catalysts into membrane electrode assemblies will require substantial efforts in the future. Extended surface materials often form poor dispersions and in select cases are magnetic (Ni, Co) further complicating mixing processes. Further efforts into optimizing coating or spraying processes will be necessary to ensure full Pt utilization in membrane electrode assemblies. A high prevalence of the template transition metal within these catalysts may also be problematic in fuel cell implementation, as the transition metal is prone to dissolution and can potentially migrate into the membrane or block catalytic sites (either at the anode or cathode). Leaching of the template metal, either in post-synthesis processing or in the electrode itself, may lower the transition metal content while maintaining high Pt utilization (surface area).

Fuel cells have the potential to fulfil clean transportation energy demands, which account for roughly one quarter of the energy consumed in the United States (26.75 quadrillion BTU in 2012).[62] Transportation needs are also expected to double for developing nations in the future (2010 – 2040).[63] The establishment of a hydrogen economy can create an entire sector of green jobs, reduce the need for petroleum imports, and eliminate the formation of greenhouse gases (when hydrogen is renewably produced).

Beyond fuel cells, galvanic displacement also holds great promise in the development of catalysts for a variety of other energy conversion devices such as electrolyzers, batteries, and solar hydrogen generators.

Notes and references

a Chemical and Materials Science Center, National Renewable Energy Laboratory, Golden, CO 80401

Email: bryan.pivovar@nrel.gov

b Department of Chemical and Biomolecular Engineering, University of Delaware, Newark, DE 19716
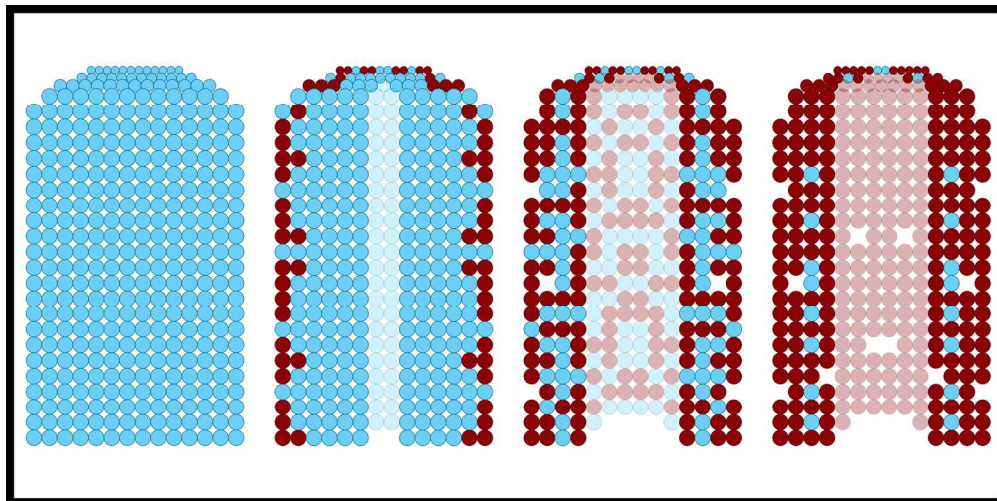
Email: yanys@udel.edu

1. H. Gasteiger, S. Kocha, B. Sompalli and F. Wagner, *Appl. Catal., B*, 2005, **56**, 9.
2. R. Darling and J. Meyers, *J. Electrochem. Soc.*, 2003, **150**, A1523.
3. R. Borup, J. Meyers, B. Pivovar, Y. Kim, R. Mukundan, N. Garland, D. Myers, M. Wilson, F. Garzon, D. Wood, P. Zelenay, K. More, K. Stroh, T. Zawodzinski, J. Boncella, J. McGrath, M. Inaba, K. Miyatake, M. Hori, K. Ota, Z. Ogumi, S. Miyata, A. Nishikata, Z. Siroma, Y. Uchimoto, K. Yasuda, K. Kimijima and N. Iwashita, *Chem. Rev.*, 2007, **107**, 3904.
4. L. J. Bregoli, *Electrochimica Acta*, 1978, **23**, 489.
5. L. Jiang, A. Hsu, D. Chu and R. Chen, *Journal of The Electrochemical Society*, 2009, **156**, B643.
6. W. Tang, H. F. Lin, A. Kleiman-Shwarscstein, G. D. Stucky and E. W. McFarland, *Journal of Physical Chemistry C*, 2008, **112**, 10515.
7. S. Alia, G. Zhang, D. Kisailus, D. Li, S. Gu, K. Jensen and Y. Yan, *Adv. Funct. Mater.*, 2010, **20**, 3742.
8. M. Debe, (Ed.: U. S. Department of Energy), http://www.hydrogen.energy.gov/pdfs/review09/fc_17_debe.pdf, 2009.
9. *M. K. Debe and E. E. Parsonage,* "Nanostructured electrode membranes",US Patent 5338430 A, 1994.
10. M. Debe, (Ed.: U. S. Department of Energy), http://www.hydrogen.energy.gov/pdfs/review08/fc_1_debe.pdf, 2008.
11. A. B. Papandrew, R. W. Atkinson, G. A. Goenaga, D. L. Wilson, S. S. Kocha, K. C. Neyerlin, J. W. Zack, B. S. Pivovar and T. A. Zawodzinski, *ECS Trans.*, 2013, **50**, 1397.
12. S. Kocha, J. Zack, S. Alia, K. Neyerlin and B. Pivovar, *ECS Trans.*, 2013, **50**, 1475.
13. Z. Chen, M. Waje, W. Li and Y. Yan, *Angew. Chem. Int. Ed.*, 2007, **46**, 4060.
14. X. Wang, W. Li, Z. Chen, M. Waje and Y. Yan, *J. Power Sources*, 2006, **158**, 154.
15. S. M. Alia, K. Duong, T. Liu, K. Jensen and Y. Yan, *ChemSusChem*, 2014, DOI: 10.1002/cssc.201400129, n/a.
16. S. M. Alia, B. S. Pivovar and Y. Yan, *J. Am. Chem. Soc.*, 2013, **135**, 13473.
17. P. Zelenay, (Ed.: U. S. Department of Energy), http://www.hydrogen.energy.gov/pdfs/review12/fc091_zelenay_2012_o.pdf, 2012.
18. Y. Sun and Y. Xia, *Adv. Mater.*, 2003, **15**, 695.
19. Y. Sun and Y. Xia, in *SPIE Proceedings*, San Diego, CA, 2003, vol. 5221, pp. 164.
20. X. Lu, M. McKiernan, Z. Peng, E. P. Lee, H. Yang and Y. Xia, *Science of Advanced Materials*, 2010, **2**, 413.

21. B. Pivovar, (Ed.: U. S. Department of Energy), http://www.hydrogen.energy.gov/pdfs/review13/fc007_pivovar_2013_o.pdf, 2013.

22. B. Pivovar, (Ed.: U. S. Department of Energy), http://www.hydrogen.energy.gov/pdfs/review12/fc007_pivovar_2012_o.pdf, 2012.

23. B. Pivovar, (Ed.: U. S. Department of Energy), http://www.hydrogen.energy.gov/pdfs/review11/fc007_pivovar_2011_o.pdf, 2011.

24. B. Pivovar, (Ed.: U. S. Department of Energy), http://www.hydrogen.energy.gov/pdfs/review10/fc007_pivovar_2010_o_web.pdf, 2010.

25. S. M. Alia, B. A. Larsen, S. Pylypenko, D. A. Cullen, D. R. Diercks, K. C. Neyerlin, S. S. Kocha and B. S. Pivovar, *ACS Catal.*, 2014, **4**, 1114.

26. S. M. Alia, S. Pylypenko, K. C. Neyerlin, D. A. Cullen, S. S. Kocha and B. S. Pivovar, *ACS Catal.*, 2014, **4**, 2680.

27. J. K. Nørskov, J. Rossmeisl, A. Logadottir, L. Lindqvist, J. R. Kitchin, T. Bligaard and H. Jónsson, *The Journal of Physical Chemistry B*, 2004, **108**, 17886.

28. A. Ruban, B. Hammer, P. Stoltze, H. L. Skriver and J. K. Nørskov, *J. Mol. Catal. A: Chem.*, 1997, **115**, 421.

29. V. Stamenkovic, B. S. Mun, K. J. J. Mayrhofer, P. N. Ross, N. M. Markovic, J. Rossmeisl, J. Greeley and J. K. Nørskov, *Angewandte Chemie*, 2006, **118**, 2963.

30. C. Koenigsmann, W.-p. Zhou, R. R. Adzic, E. Sutter and S. S. Wong, *Nano Lett.*, 2010, **10**, 2806.

31. N. R. Jana, L. Gearheart and C. J. Murphy, *Chem. Commun.*, 2001, DOI: 10.1039/b100521i, 617.

32. Z. Liu, Y. Yang, J. Liang, Z. Hu, S. Li, S. Peng and Y. Qian, *J. Phys. Chem. B*, 2003, **107**, 12658.

33. I. Pastoriza-Santos, A. Sánchez-Iglesias, B. Rodríguez-González and L. M. Liz-Marzán, *Small*, 2009, **5**, 440.

34. K. R. Krishnadas, P. R. Sajanlal and T. Pradeep, *J. Phys. Chem. C*, 2011, **115**, 4483.

35. Y. Leng, Y. Li, X. Li and S. Takahashi, *J. Phys. Chem. C*, 2007, **111**, 6630.

36. B.-Q. Xie, Y. Qian, S. Zhang, S. Fu and W. Yu, *Eur. J. Inorg. Chem.*, 2006, **2006**, 2454.

37. E. Vargas, P. Toro, J. Palma, J. Escrig, C. Chanéac, T. Coradin and J. Denardin, *Mater. Lett.*, 2013, **94**, 121.

38. J. Zhang, Y. Mo, M. B. Vukmirovic, R. Klie, K. Sasaki and R. R. Adzic, *Journal of Physical Chemistry B*, 2004, **108**, 10955.

39. M. Mavrikakis, J. L. Zhang, M. B. Vukmirovic, Y. Xu and R. R. Adzic, *Angewandte Chemie-International Edition*, 2005, **44**, 2132.

40. R. R. Adzic, M. Shao, K. Sasaki, N. S. Marinkovic and L. Zhang, *Electrochemistry Communications*, 2007, **9**, 2848.

41. S. R. Brankovic, J. X. Wang and R. R. Adžić, *Surf. Sci.*, 2001, **474**, L173.

42. Y. Xia, P. Yang, Y. Sun, Y. Wu, B. Mayers, B. Gates, Y. Yin, F. Kim and H. Yan, *Adv. Mater.*, 2003, **15**, 353.

43. B. Larsen, K. Neyerlin, J. Bult, C. Bochert, J. Blackburn, S. Kocha and B. Pivovar, *J. Electrochem. Soc.*, 2012, **159**, F622.

44. S. Alia, K. Jensen, B. Pivovar and Y. Yan, *ACS Catal.*, 2012, **2**, 858.

45. S. Alia, K. Jensen, C. Contreras, F. Garzon, B. Pivovar and Y. Yan, *ACS Catal.*, 2013, **3**, 358.

46. J. R. Varcoe and R. C. T. Slade, *Fuel Cells*, 2005, **5**, 187.

47. K. C. Neyerlin, W. Gu, J. Jorne and H. A. Gasteiger, *Journal of The Electrochemical Society*, 2007, **154**, B631.

48. V. S. Bagotzky and N. V. Osetrova, *Journal of Electroanalytical Chemistry and Interfacial Electrochemistry*, 1973, **43**, 233.

49. J. S. Spendelow and A. Wieckowski, *Physical Chemistry Chemical Physics*, 2007, **9**, 2654.

50. S. M. Alia, K. Duong, T. Liu, K. Jensen and Y. Yan, *ChemSusChem*, 2012, **5**, 1619.

51. B. B. Blizanac, P. N. Ross and N. M. Markovic, *Journal of Physical Chemistry B*, 2006, **110**, 4735.

52. *Y. Yan and S. M. Alia,* "Extended Two Dimensional Metal Nanotubes and Nanowires Useful as Fuel Cell Catalysts and Fuel Cells Containing the Same", WO Patent 2012064768, 2012.

53. R. R. Adzic, A. V. Tripkovic and N. M. Markovic, *Journal of Electroanalytical Chemistry*, 1983, **150**, 79.

54. K. Juttner, *Electrochimica Acta*, 1984, **29**, 1597.

55. S. Strbac and R. R. Adzic, *Journal of Electroanalytical Chemistry*, 1996, **403**, 169.

56. M. H. Shao, P. Liu, J. L. Zhang and R. Adzic, *Journal of Physical Chemistry B*, 2007, **111**, 6772.

57. A. Kowal, M. Li, M. Shao, K. Sasaki, M. B. Vukmirovic, J. Zhang, N. S. Marinkovic, P. Liu, A. I. Frenkel and R. R. Adzic, *Nat Mater*, 2009, **8**, 325.

58. J. K. Nørskov, T. Bligaard, A. Logadottir, J. R. Kitchin, J. G. Chen, S. Pandelov and U. Stimming, *Journal of The Electrochemical Society*, 2005, **152**, J23.

59. D. Strmcnik, M. Uchimura, C. Wang, R. Subbaraman, N. Danilovic, V. van der, A. P. Paulikas, V. R. Stamenkovic and N. M. Markovic, *Nat Chem*, 2013, **5**, 300.

60. A. V. Tripkovic, K. D. Popovic, B. N. Grgur, B. Blizanac, P. N. Ross and N. M. Markovic, *Electrochimica Acta*, 2002, **47**, 3707.

61. E. H. Yu and K. Scott, *Journal of Power Sources*, 2004, **137**, 248.

62. U. S. Energy Information Administration, http://www.eia.gov/totalenergy/data/annual/index.cfm, 2012.

63. U. S. Energy Information Administration, http://www.eia.gov/forecasts/ieo/transportation.cfm, 2013.

Catalysis Science & Technology Accepted Manuscript

846x423mm (72 x 72 DPI)